11th Australasian Fluid Mechanics Conference
University of Tasmania, Hobart, Australia
14-18 December 1992

THREE-COMPONENT AERODYNAMIC FORCE MEASUREMENTS IN HYPERVELOCITY IMPULSE FACILITIES

D.J. MEE, W.J. DANIEL and J.M. SIMMONS

Department of Mechanical Engineering
University of Queensland
QLD 4072, AUSTRALIA

ABSTRACT

This paper describes a balance for the measurement of three force components in hypervelocity flow - lift, drag and the associated pitching moment. The balance is proposed for use in impulse aerodynamic facilities where the test time may be 1 ms or less. The technique is an extension of the drag balance developed at The University of Queensland for measurements in the T4 shock tunnel. The new balance has been designed using dynamic finite element programs to determine the propagation and reflection of stress waves within the model and an attached sting. A deconvolution procedure is used to determine the model loadings from the strains in the coupling between the model and a sting and in the sting itself.

NOTATION

g,G,G	Impulse response - time history, matrix, Fourier transform
t	Time
$u,\boldsymbol{u},U$	Input load - time history, vector, Fourier transform
$y,\boldsymbol{y},Y$	Output signal - time history, vector, Fourier transform
ε	Axial strain
ω	Angular frequency
Subscripts	
D	Drag
L	Lift
M	Pitching moment
U,V,X,Y,Z	Refer to Figure 5

1. INTRODUCTION

The design of vehicles for flight at hypervelocity conditions relies on the prediction of forces acting on the vehicle. The stability and manoeuvrability are dependent on the magnitude and line of action of these forces (Kremer, 1992). Ground facilities capable of simulating flows representative of flight at such conditions typically produce test times which may be as short as 1 ms in duration (Stalker and Morgan, 1988). There is also the prospect that future expansion tubes with free-piston drivers will produce higher flow speeds (up to 10 km/s, Neely et al., 1991) with associated lower test times (hundreds of microseconds).

Conventional techniques for force measurements in wind tunnels are found to be unsuitable for flows with test times of the order of milliseconds (Bernstein, 1975; Sanderson and Simmons, 1991). In order for the model to reach a static equilibrium with a strain-gauged sting during the test time, the model and sting must be made prohibitively light and short. For free-flight techniques to be successful the model again must be made very light in order that high accelerations can produce detectable movement within the test time. A balance technique has been developed which overcomes these restrictions and enables drag to be measured successfully during a millisecond of steady flow.

In this paper the deconvolution approach to measurement of drag in short-duration shock tunnels is summarised in order that the three-component balance may be introduced. Certain practical considerations for multiple-component balances, such as time-domain versus frequency-domain deconvolution, are addressed. The design of the lift, drag and pitching moment balance is then presented.

2. THE DECONVOLUTION FORCE BALANCE

The single force component measurement technique developed at The University of Queensland (Sanderson and Simmons, 1991) involves monitoring stress waves as they pass a location on a sting attached to the base of the model (Fig. 1). These stress waves, produced by the rapid application of aerodynamic loads, propagate and reflect within the model and sting. As indicated in the figure, the balance arrangement is suspended to allow free movement in the plane of the drag force. The sting, approximately 2 m in length, is shielded from any aerodynamic load. From the model and sting geometry and the form of aerodynamic loading on the model, an impulse response is determined to relate the stress in the sting to the applied loading. This impulse response can be found by means of dynamic finite element analysis or bench tests in which weights are attached to the model by fine wires and are suddenly released to produce a step change in the load.

The stresses in the sting are measured during a shot of the tunnel. The loading in The University of Queensland T4 shock tunnel typically takes the form of a rapid rise as the

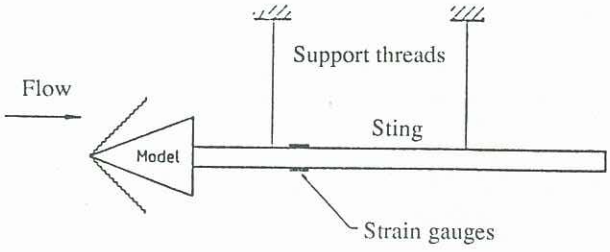

Figure 1 Arrangement of drag balance.

tunnel starting processes take place followed by a decrease to the true drag level as the flow becomes established. The drag level then remains essentially constant if the tunnel is operated in tailored mode or slowly decreases with time for under-tailored operation. This loading history is reflected in the Pitot pressure trace for the run, an example of which is given for a tailored shot in Figure 2. The starting processes last for approximately 0.5 ms. They are followed by a test time of approximately 1 ms which is terminated when the test gas is contaminated by the helium driver gas.

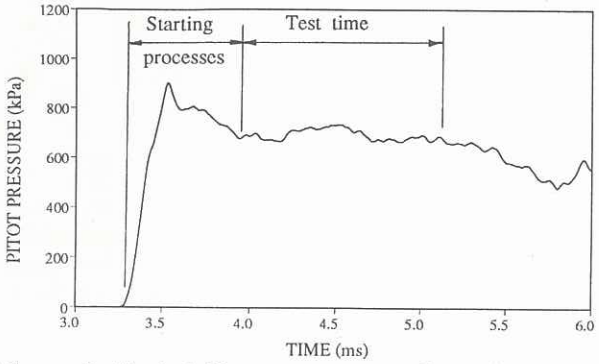

Figure 2 Typical Pitot pressure trace for a shot of T4 (tailored condition).

The stress measured in the sting during the tunnel shot, $y(t)$, is related to the time-history of the load applied to the model, $u(t)$, and the impulse response for the model/sting configuration, $g(t)$, via a convolution integral of the form,

$$y(t) = \int_0^t g(t-\tau)\, u(\tau)\, d\tau. \qquad (1)$$

The procedure for determining the applied loading from the measured output is referred to as deconvolution. This can be performed most elegantly in the frequency domain by taking Fourier Transforms of $g(t)$ and $y(t)$, referred to as $G(\omega)$ and $Y(\omega)$ respectively. Then the convolution integral of the time domain becomes a simple multiplication in the frequency domain. The transform of the applied load, $U(\omega)$, is found by

$$U(\omega) = Y(\omega) / G(\omega) \qquad (2)$$

The loading on the model during the shot is then determined by taking the inverse Fourier transform. The deconvolution procedure is very sensitive to noise and Wiener filtering was found to be necessary in cases where the signal-to-noise ratio was high (Sanderson and Simmons, 1991). However, for smaller signal-to-noise ratios heavier filtering was found to be necessary in order to obtain an adequate signal (Tuttle and Simmons, 1992). A result for the drag measured on a 15° semi-angle cone at Mach 6.9 for a stagnation enthalpy of 4.0 MJ/kg is given in Figure 3. The drag on the cone is predicted using the theory outlined in Taylor and Maccoll (1932). Agreement with the measurements is good.

2.1 Time-domain Deconvolution

The frequency-domain approach to deconvolution is suitable when the impulse response is time limited during the length of the steady test time (i.e. the impulse response is non-zero for only a limited extent). If that is not the case then the cyclic nature of the transform can lead to errors in

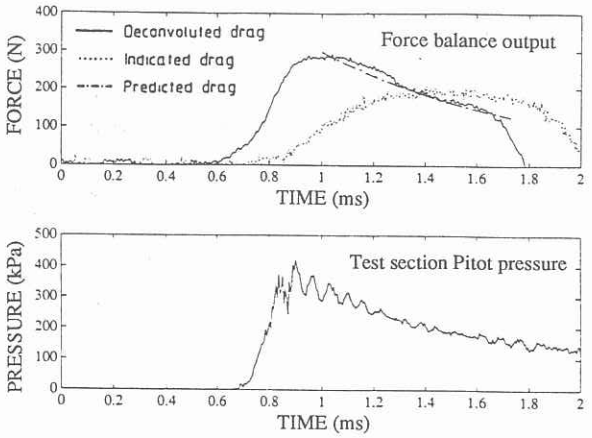

Figure 3 Sample result for drag balance performance. 15° cone; Mach 6.9; 4.0 MJ/kg stagnation enthalpy; under-tailored condition.

the deconvolved signal. An alternative approach to the deconvolution is to work in the time domain so that such problems can be avoided. This is done at the cost of a much greater time for computation. The time domain also has the advantage that constraints can be applied to the deconvolved signal during an iteration procedure (Prost and Goutte, 1984).

When the data are discretised, (1) can be written in matrix notation as

$$\boldsymbol{y} = \boldsymbol{G}\,\boldsymbol{u} \qquad (3)$$

where $\boldsymbol{y}$ is the vector formed from the stains measured in the sting at each point in time and $\boldsymbol{G}$ is a square matrix formed from the impulse response. $\boldsymbol{u}$ is then the vector of the applied loading. Direct solution techniques for this are ill-conditioned and iterative procedures are used (eg. Prost and Goutte, 1984). Time-domain deconvolution has been used in testing designs for the multi-component force balance.

3. THREE-COMPONENT FORCE BALANCE

3.1 Coupled Deconvolution

When three components of force are required, three strain output histories must be measured. Ideally these outputs are independent. The outputs related to the lift force, drag force and pitching moment are labelled $y_L(t)$, $y_D(t)$ and $y_M(t)$ respectively. Three, one-dimensional deconvolutions will then reproduce the three applied load histories. For practical balance designs there will be some coupling amongst the outputs. Thus, for example, a pure lift force may produce a non-zero output on the y_D and/or y_M signals in addition to an output on the y_L signal. This can be accounted for by determining nine impulse responses relating each of the three output signals to each of the three applied load signals. Forming vectors from the time signals as in Section 2, the relationship between the input and output signals can be written in vector notation as

$$\begin{bmatrix} y_L \\ y_D \\ y_M \end{bmatrix} = \begin{bmatrix} G_{LL} & G_{LD} & G_{LM} \\ G_{DL} & G_{DD} & G_{DM} \\ G_{ML} & G_{MD} & G_{MM} \end{bmatrix} \begin{bmatrix} u_L \\ u_D \\ u_M \end{bmatrix} \qquad (4)$$

where the $\boldsymbol{y}$ vectors are formed from the discretised time signals, the $\boldsymbol{u}$ vectors are formed from the applied loads and the subscripts for these vectors are as described above. The

square G submatrices are formed from the impulse responses, G_{ij} being the impulse response for the y_i output to a u_j input. If there is no coupling amongst the outputs then the off-diagonal submatrices of the impulse response matrix in (4) will be null. The time-domain deconvolution techniques described in Section 2.1 can be applied to (4).

3.2 Finite Element Analysis

The designs for the multi-component force balance have been analysed using the finite element program MSC/NASTRAN Version 66 (Reymond, 1991). This package can be used to analyse the dynamics of one-, two- and three-dimensional models. Some models were analysed with another package for three-dimensional models, DYNA3D (Whirley, 1991). For a given design, the strain history at any point on the model or sting can be determined. Impulse responses are found by predicting the strain histories at the proposed locations of strain gauge bridges for a step application of load. Differentiation of these strain signals with respect to time gives the impulse responses. In order to test the design, the finite element package is used to predict the strains for a loading representative of that experienced by the model during a shot of the shock tunnel. The output strain histories are then deconvolved using the predicted impulse responses to try to reproduce the applied loads. These deconvolved loads are then compared with the actual applied loads to assess the effectiveness of the force balance design.

3.3 Balance Design

It is theoretically possible to determine three aerodynamic force components on a model with the same balance geometry that was used for the single component balance of Figure 1. If measurements are made of the axial, bending and transverse shear strain histories at a point on the sting then a coupled deconvolution procedure could be used to determine the applied loads. Such a measurement technique has been simulated with a two-dimensional finite element model. The simulated output signals were deconvolved to produce a representation of the applied load as described in Section 3.2. The drag signal, which is determined from the axial strain, is assumed to be decoupled from the lift and moment signals. The results are shown in Figure 4 where it is seen that the general form of the applied lift and pitching moment loads have been reproduced although the signals are quite noisy.

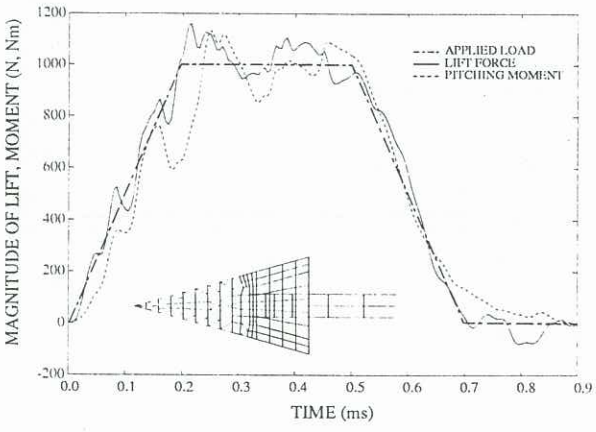

Figure 4 Predicted performance of arrangement of Fig. 1 for measurement of coupled lift and pitching moment applied loads. Inset is the finite element grid used.

A difficulty with this approach is that, for typical loading distributions, the bending strains in the sting will be much larger in magnitude than the other strains. This will make practical measurement of axial and shear strain time histories very difficult and deconvolution will amplify uncertainties in the strains. Another consideration is that bending, or flexural, waves travel at speeds dependent on their wavelength and thus tend to disperse as they travel, whereas the speed of propagation of axial stress waves is independent of wavelength (Kolsky, 1963). There is also a loss of high frequency information in using bending signals.

The present design for the three-component balance involves only the measurement of axial strains with a single sting arrangement. This is achieved by measuring the strains in four mounting bars between the sting and the model. The design is shown schematically in Figure 5. The output signals are derived from measurement of axial strain in the four members connecting the sting to the model as well as the axial strain in the sting. The mounting bars in the force balance device are labelled in Figure 5. The drag output, $y_D(t)$, is the strain in the sting at point Z, $\varepsilon_Z(t)$, as in the drag balance of Section 2. The lift output, $y_L(t)$, is given by

$$y_L(t) = \{\varepsilon_U(t) + \varepsilon_V(t)\} - \{\varepsilon_X(t) + \varepsilon_Y(t)\} \quad (5)$$

and the moment output, $y_M(t)$, is given by

$$y_M(t) = \{\varepsilon_U(t) - \varepsilon_V(t)\} - \{\varepsilon_X(t) - \varepsilon_Y(t)\}. \quad (6)$$

This selection of outputs reduces the coupling amongst the signals.

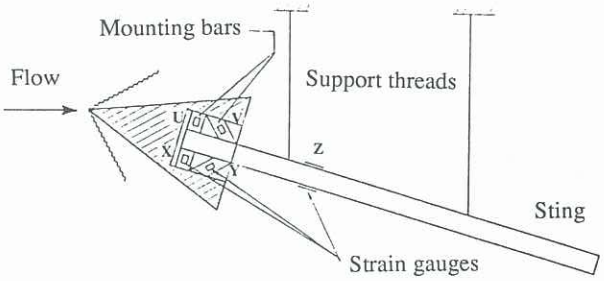

Figure 5 Design of prototype three-component force balance.

A sample impulse response for this configuration, $g_{LL}(t)$, is given in Figure 6. As is typical for this device, the impulse response is quite oscillatory. The time at which the reflection from the end of the sting arrives back at the measurement location depends on the length of the sting. This length is governed by the wind tunnel geometry and the angle of attack of the model. For a 3D finite element representation of this design, Figure 7 shows an example of the results of deconvolution for coupled lift and pitching moment applied loads. It can be seen that the deconvolved results reproduce the input loading very well, although the signals are noisy in the first 150 μs.

A prototype three-component balance has been manufactured and has undergone preliminary bench testing. Figure 8 shows an example of the measured output voltage (from a strain gauge bridge located on mounting bar V of the balance) for a step application of a drag-type load. The step change of load was obtained by cutting a fine wire attaching an 18 kg mass to the model. The result is compared with the strain history predicted from the 3D finite element model. It can be seen that there is good agreement in the timing of

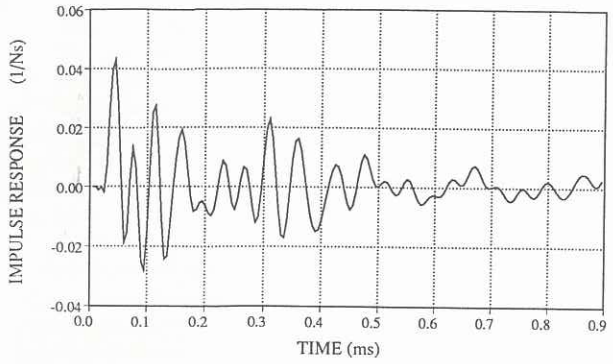

Figure 6 Impulse response, $g_{LL}(t)$, for prototype design.

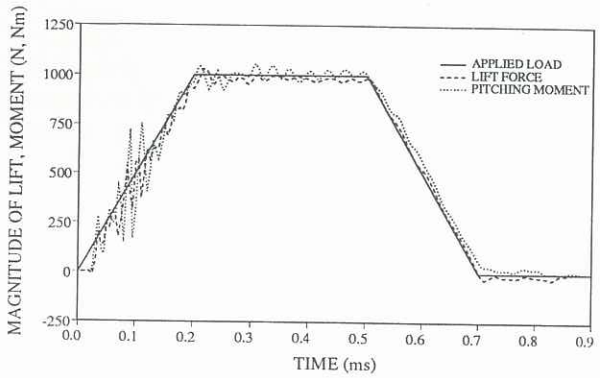

Figure 7 Predicted performance of prototype design for coupled lift and moment applied loads.

stress wave patterns in the balance. Further testing is in progress and it is proposed to validate the balance by measuring the forces on a cone at angle of attack in the T4 shock tunnel.

CONCLUSIONS

A new force balance for measurement of the three aerodynamic components, lift, drag and pitching moment, has been presented. The balance is based on an extension of an existing single component device and is designed to measure forces in impulsively starting hypervelocity flows with test times of 1 ms or less. The prototype has been designed using dynamic finite element analysis in conjunction with numerical deconvolution techniques. Simulations indicate that the device presented will be capable of simultaneous measurement of the three force components and initial tests confirm the finite element modelling.

ACKNOWLEDGEMENTS

The authors are grateful for the support received from the Australian Research Council under grant AE9032029 and the Queen Elizabeth II Fellowship Scheme (for Dr. D. Mee).

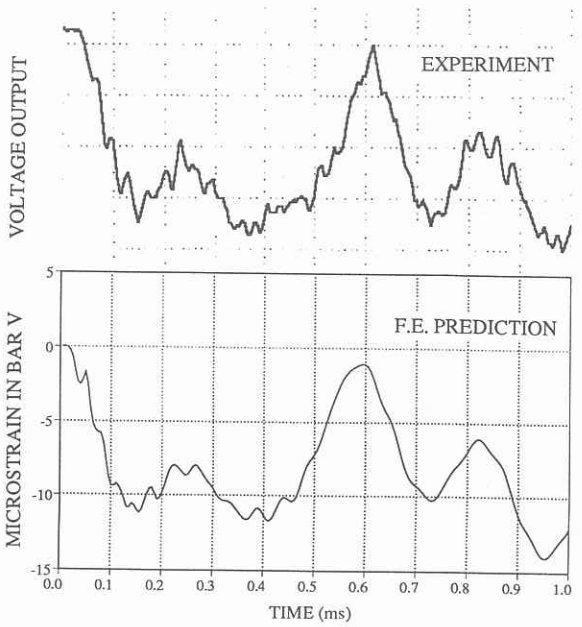

Figure 8 Measured and predicted response of prototype design to a step application of a drag-type load.

REFERENCES

BERNSTEIN, L. (1975) Force measurements in short-duration hypersonic facilities. AGARDograph No. 214.

KOLSKY, H. (1963) Stress waves in solids. Dover Publications. New York.

KREMER, F.G.J (1992) Balance of moments for hypersonic vehicles. ASME Paper No. 92-GT-251.

NEELY, A.J., STALKER, R.J. and PAULL, A. (1991) High enthalpy, hypervelocity flows of air and argon in an expansion tube. Aero J, 95, 175-186.

PROST, R. and GOUTTE, R. (1984) Discrete constrained iterative deconvolution algorithms with optimized rate of convergence. Signal Process, 7, 209-230.

REYMOND, M.A. (1991) MSC/NASTRAN Users Manual. MacNeal-Schwendler Corporation. August 1991.

SANDERSON, S.R and SIMMONS, J.M (1991) Drag balances for hypervelocity impulse facilities. AIAA J, 29, 278-297.

STALKER, R.J. and MORGAN, R.G. (1988) Free piston shock tunnel T4 - initial operation and preliminary calibration. NASA CR-181721.

TAYLOR, G.I. and MACCOLL, J.W. (1932) The air pressure on a cone moving at high speed - II. Proc Roy Soc (Lond), Ser A, 139, 298-311.

TUTTLE, S.L. and SIMMONS, J. M. (1992) Hypersonic drag measurements in free piston shock tunnels. Proc. 11th Australasian Fluid Mech Conf, Hobart.

WHIRLEY, R.G. (1991) DYNA3D Users Manual. Lawrence Livermore National Laboratory, Report UCRL-MA-107254.